Multi-wavelength high-order optical vortex detection and demultiplexing coding using a metasurface

Dahai Yang, [a,b] Jie Lin, [a,c,*], Chen Chen, [d] Chang Li, [d] Junbo Hao, [a,b] Baiying Lv, [d] Keya Zhou, [c] Yiqun Wang, [d] and Peng Jin [a,b **]

[a] Key Laboratory of Micro-systems and Micro-structures Manufacturing (Harbin Institute of Technology), Ministry of Education, Harbin 150001, China

[b] School of Instrumentation Science and Engineering, Harbin Institute of Technology, Harbin 150001, China

[c] School of Physics, Harbin Institute of Technology, Harbin 150001, China

[d] Suzhou Institute of Nano-Tech and Nano-Bionics, Chinese Academy of Sciences, Suzhou 215125, China

* Corresponding authors: P.Jin@hit.edu.cn ; linjie@hit.edu.cn

Supplementary material:

Supplementary material 1.

The saddle-shaped phase (SSP) is derivated by the orthogonal Double cylinder lens. Using geometric optics, one can obtain the phase expression of SSP. In physical optics, there is a model of the equal thickness interference. Here, the equal-thickness interference between orthogonal cylindrical lenses is reviewed.

1) As shown in Figure.S1, the plano-convex cylindrical lens is tangent to the flat glass. In a right triangle with sides *R*, *R-e*, and *r*, there is $R^2 = (R-e)^2 + r^2$, which is simplified $2Re - e^2 = r^2$. Therefore, when the plano-convex cylindrical lens is tangent to the plate glass (the plane section of the cylindrical lens is parallel to the plate). The light is incident perpendicularly on the paraxial axis. The thickness of the air gap is much smaller than the cylindrical radius, that is $e \ll R$. There is the following formula,

$$e = \frac{r^2}{2R}. \tag{S1-1}$$

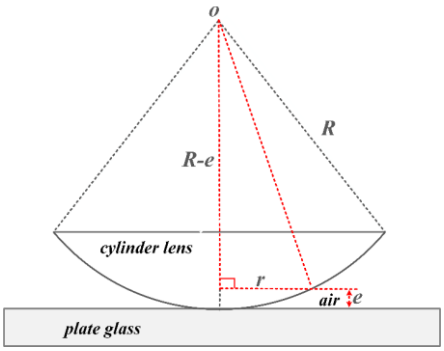

Figure S1. Axial side view of geometric model with plano-convex cylindrical lens tangent to flat glassthe.

2) As shown in Figure S2, the plano-convex cylindrical lens and the plano-convex cylindrical lens are orthogonally tangent. The Equation (S1-1) is satisfied based on the paraxial approximation condition. The two plano-convex cylindrical lenses are placed back-to-back tangentially. The plane cross-sections of the two lenses are parallel to each other, and the symmetry axes

are perpendicular to each other, as shown in Figure S2. When the beam with wavelength λ is perpendicularly incident along the z-axis direction. The interference of equal thickness will be occur between the two cylindrical surfaces.The expected elliptical Newton ring pattern can be observed with the uniform thickness stripes formed.

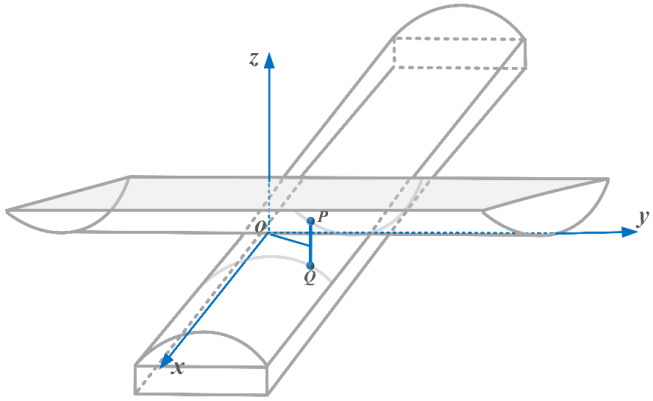

Figure S2. Axial side view of the geometric model of the plano-convex cylindrical lens tangent to the plano-convex cylindrical lens

As shown in Figure S2, the point *o* is selected as the origin of the space rectangular coordinate system *o*-*x*-*y*-*z* between the two cylinders. The *x*-axis is the side cylinder (radius R_2) and the generatrix of the tangent point *o*. The generatrix of the cross-cut point *o* of the upper cylindrical surface (radius R_1) is as the y-axis. Point P and Q are on the upper and lower cylinders, respectively. PQ is perpendicular to the *x*-*o*-*y* plane and parallel to the *z* axis. The coordinates of points P and Q are P(x, y, z_p), Q(x, y, z_Q), respectively.

According to the condition of paraxial vertical incidence and the relational formula (S1-1), the distances from the two points P and Q to the *x*-*o*-*y* tangent plane are

$$e_1 = z_p = \frac{r_x^2}{2R_1} = \frac{x^2}{2R_1}, \tag{S1-2}$$

$$e_2 = -z_Q = \frac{r_y^2}{2R_2} = \frac{y^2}{2R_2}. \tag{S1-3}$$

where, r_x=x; r_y=y are the distances from point P to the *z*-*o*-*y* plane and point Q to the *z*-*o*-*x* plane, respectively. n_0 is assumed the refractive index of the medium between the cylinders (for example: air refractive n_0=1.0). The reflected optical path difference of the incident light with the vacuum wavelength λ between the two cylinders is as following,

$$\begin{aligned} \Delta L &= 2n_0\left(z_p - z_Q\right) + \lambda/2 \\ &= 2n_0\left(e_1 + e_2\right) + \lambda/2 \\ &= n_0\left(\frac{x^2}{R_1} + \frac{y^2}{R_2}\right) + \frac{\lambda}{2} \end{aligned}. \tag{S1-4}$$

On the *x*-*o*-*y* plane, the projection point (x, y) of the two PQ points will be falls on the *k*-th bright (or dark) pattern, the condition of ΔL must meet

$$\Delta L = n_0\left(\frac{x^2}{R_1} + \frac{y^2}{R_2}\right) + \frac{\lambda}{2} = \begin{cases} k\lambda, k \in N, (x, y) & \text{the } k\text{-th light streak;} \\ \left(k + \frac{1}{2}\right)\lambda, k \in N, (x, y) & \text{the } k\text{-th dark streak.} \end{cases} \tag{S1-5}$$

Here, assuming k=1, and R_1=R_2=R>0, which can be obtained from the formulas (S1-4) and (S1-5),

$$\frac{x^2}{\frac{R\lambda}{n}}+\frac{y^2}{\frac{R\lambda}{n}}=1. \tag{S1-6}$$

If k=1, and assuming R_1=R>0, R_2=R<0, one can obtain

$$\frac{x^2}{\frac{R\lambda}{n_0}}-\frac{y^2}{\frac{R\lambda}{n_0}}=1. \tag{S1-7}$$

The fringes shown in formula (S1-7) are hyperbolic. It is equivalent to the coherence of a plano-convex lens with a plano-concave lens. To simplify the expression, for F = $n_0/\lambda R$, it is F(x^2-y^2) = 1.

Based on Equation (S1-7), a rotation angle θ is introduced to allow the hyperbola to rotate arbitrarily in the coordinate plane. Rotation formula is as

$$\begin{pmatrix} x \\ y \end{pmatrix}=\begin{pmatrix} \cos\theta & -\sin\theta \\ \sin\theta & \cos\theta \end{pmatrix}\begin{pmatrix} x \\ y \end{pmatrix}. \tag{S1-8}$$

Substituting the rotated coordinates in formula (S1-8) into formula (S1-7), one can obtain

$$\left(x\cos\theta-y\sin\theta\right)^2-\left(x\sin\theta+y\cos\theta\right)^2=1/F. \tag{S1-9}$$

Then,

$$F\bullet\left[\left(x^2-y^2\right)\cos 2\theta-2xy\sin 2\theta\right]=1. \tag{S1-10}$$

Therefore, the orthogonal double cylindrical lens saddle-shaped phase distributionas can be written as following,

$$\psi\left(x,y,\theta\right)=\mathrm{F}\bullet\left[\left(x^2-y^2\right)\cos 2\theta-2xy\sin 2\theta\right]. \tag{S1-11}$$

Supplementary material 2.

2D and 3D SSP distribution pattern with different F numbers and a rotation angle θ.

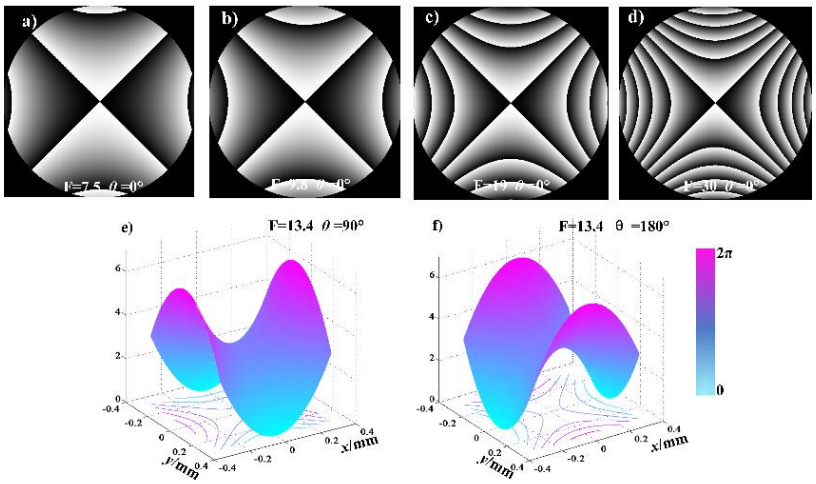

Figure S3. SSP 2D and 3D distribution pattern under different F numbers.

a) F=7.5mm^{-2}, the corresponding waist value is 0.2mm. b)F=9.8mm^{-2}, the corresponding waist value is 0.25mm.

c) F=19mm^{-2}, the corresponding waist value is 0.35mm. d)F=30mm^{-2}, the corresponding waist value is 0.40mm.

e) 3-D phase distribution and the corresponding isophase line of SSP for F=13.4mm^{-2}, θ=90°.

f) 3-D phase distribution and the corresponding isophase line of SSP for F=13.4mm^{-2}, θ=180°(or 0°).

In the Figure S3, the corresponding SSP phase distribution fringes will be increasing with the increasing F parameter.

Supplementary material 3.

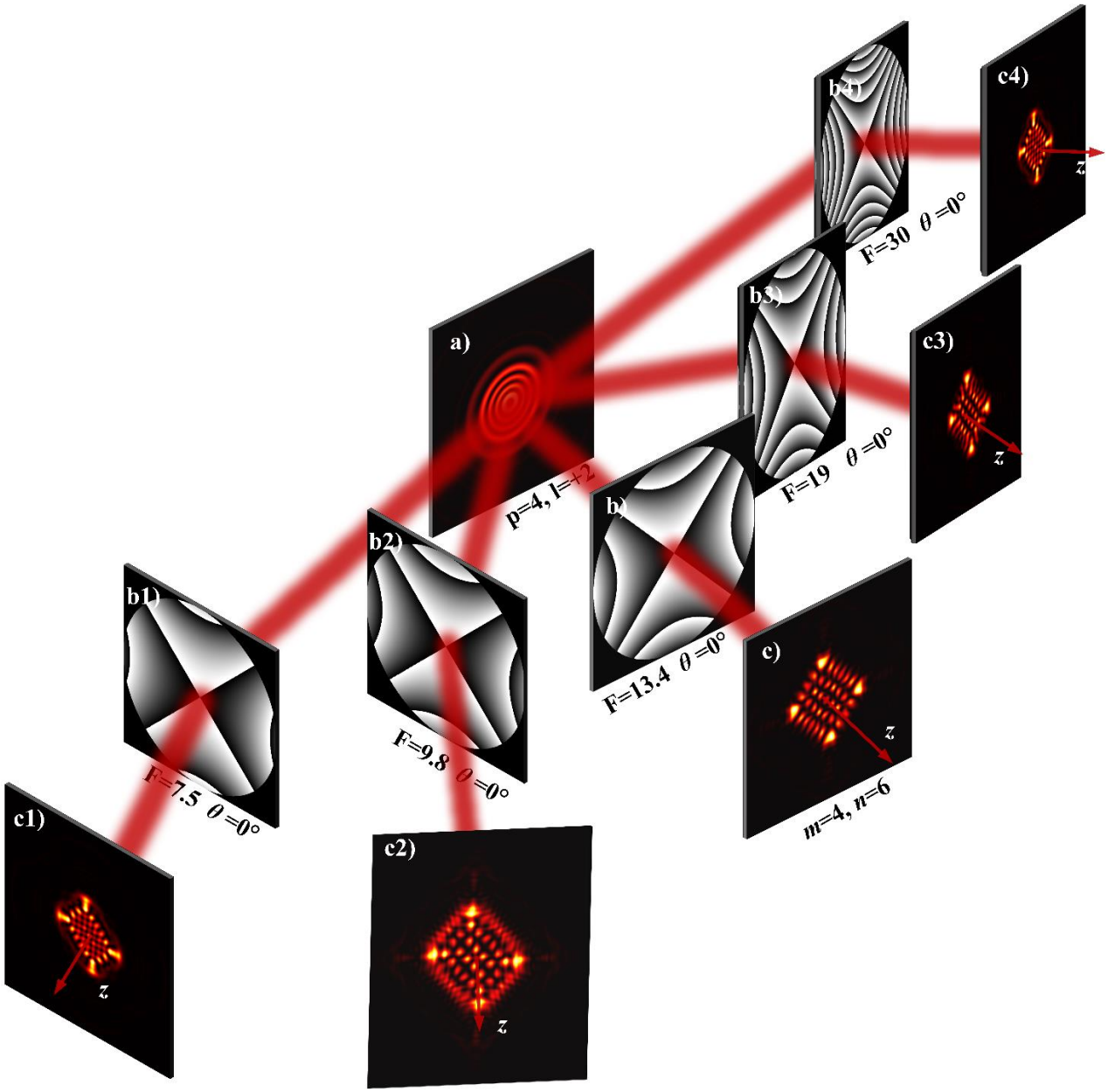

Figure S4. Conversion of SSP to $LG_{4,2}$ in the different F parameters

a) The incident field $LG_{4,2}$. b1)-b4) SSP phase corresponding to different F parameters.

c1)-c4) The conversion results of the incident field $LG_{4,2}$ under different SSP F parameters.

Figure S4 is a schematic of $LG_{4,2}$ modulated by SSP with different F-number. From a) - c), one can accurately realize the detection between the two modes. The incident field $LG_{4,2}$ can be effectively demodulated only under the corresponding F-parameter modulation. The modulation with different F parameters will produce a light field distribution called generalized Higher Laguerre-Gauss mode, which is shown in Figures S4.c1), c2), c3), and c4). Therefore, through the setting F parameter, a rich and colorful special optical field distribution can be achieved.

Supplementary material 4.

The conversion efficiency of a single nanorods in a metasurface and the phase modulation relationship, for three wavelengths of the PB phase rotation angle.

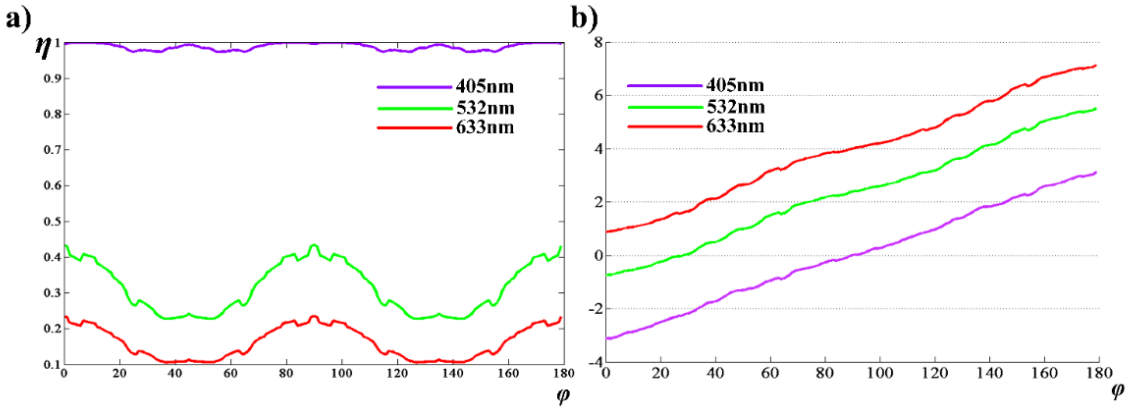

Figure S5. a) The energy conversion efficiency of a single nanorods at three wavelengths.

b) The phase modulation curve corresponding to the PB phase rotation angle at three wavelengths.

Figure S5. a) is the energy conversion efficiency of a single nanorod at three wavelengths. The blue purple curve represents the conversion efficiency of a single nanorods at the design wavelength of 405nm. For the angle of 0-π, the energy conversion efficiency of a single nanorods can be ≥98%. For the green curve wavelength of 532nm and the red curve wavelength of 633nm, the maximum energy conversion efficiency are larger than 42% and 22%. Figure S5. b) shows the relationship between the corresponding PB phase rotation angle and the phase modulation for the three wavelengths. The wavelength corresponds to the color of a curve. Through the modulation curve, between the phase rotation angles of 0-π, the phase modulation range corresponding to the three wavelengths is between 0-2π.

Supplementary material 5.

Photos of metasurface devices.

Figure S6. Metasurface sample image.

Figure S6. is the actual photo of the fabricated sample of metasurface. The diameter of the wafer is 5 cm. The red circle is

the fabricated metasurface. The diameter of the gold film is 6mm. The metasurface structure is in a circular area with a diameter of 600um. The specific processing technology can refer to our previous works.

Supplementary material 6.

Test optical path.

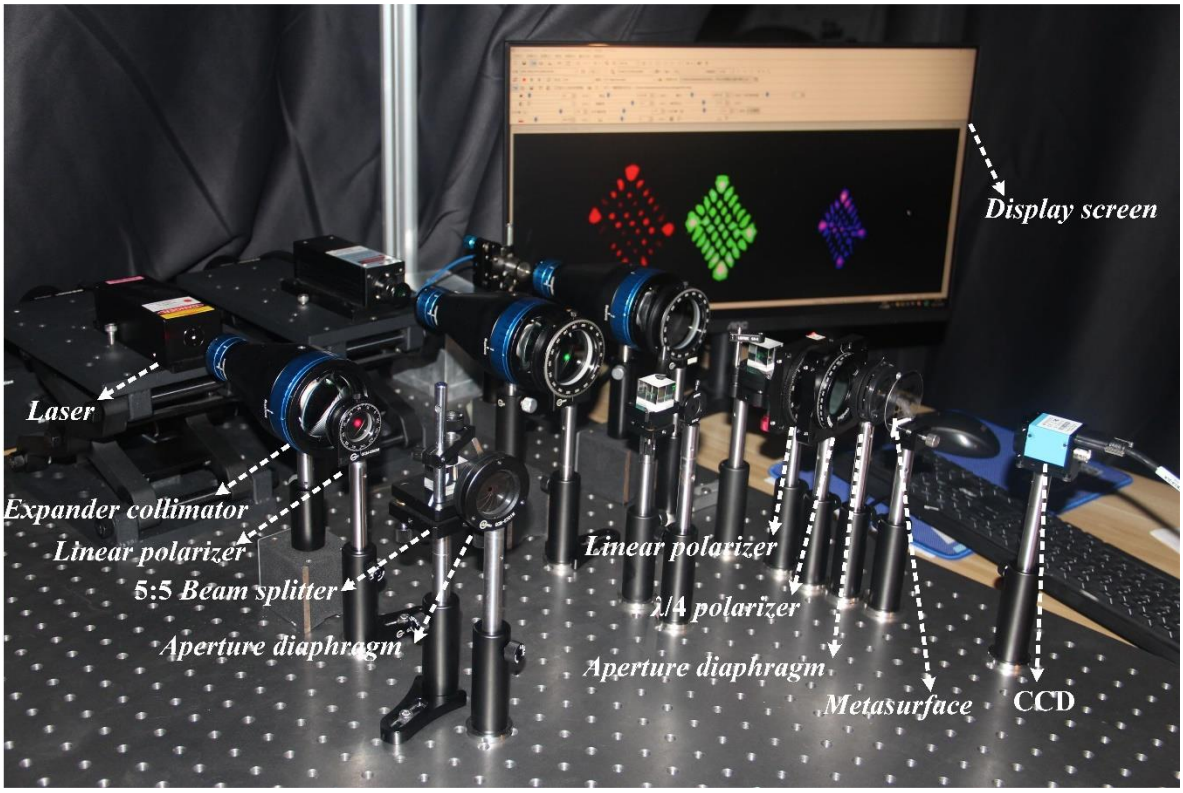

Figure S7. Sample measured three-wavelength beam combining experimental device.

Figure S7 is the test optical path of metasurface. It will carry out the beam combining experiment of multiple wavelengths. The experiments were often done at a single wavelength with the previously reported experiments on structured beam based on metasurfaces.